LAWRENCE
LIVERMORE
NATIONAL
LABORATORY

UCRL-JRNL-236545

Three dimensional modeling of Laser-Plasma interaction: benchmarking our predictive modeling tools vs. experiments

L. Divol, R. Berger, N. Meezan, D. H. Froula, S. Dixit, L. Suter, S. H. Glenzer

November 14, 2007

Physics of Plasma

Disclaimer

Three dimensional modeling of Laser-Plasma interaction: benchmarking our predictive modeling tools vs. experiments

L. Divol, R. L. Berger, N. B. Meezan, D. H. Froula, S. Dixit, L. Suter and S. H. Glenzer
L-399, Lawrence Livermore National Laboratory,
University of California P. O. Box 808, CA 94551, U.S.A.
(Dated: November 9, 2007)

We have developed a new target platform to study Laser Plasma Interaction in ignition-relevant condition at the Omega laser facility (LLE/Rochester)[1]. By shooting an interaction beam along the axis of a gas-filled hohlraum heated by up to 17 kJ of heater beam energy, we were able to create a millimeter-scale underdense uniform plasma at electron temperatures above 3 keV. Extensive Thomson scattering measurements allowed us to benchmark our hydrodynamic simulations performed with HYDRA[2]. As a result of this effort, we can use with much confidence these simulations as input parameters for our LPI simulation code pF3d[3]. In this paper, we show that by using accurate hydrodynamic profiles and full three-dimensional simulations including a realistic modeling of the laser intensity pattern generated by various smoothing options, whole beam three-dimensionnal linear kinetic modeling of stimulated Brillouin scattering reproduces quantitatively the experimental measurements(SBS thresholds, reflectivity values and the absence of measurable SRS). This good agreement was made possible by the recent increase in computing power routinely available for such simulations. These simulations accurately predicted the strong reduction of SBS measured when polarization smoothing is used.

PACS numbers: PACS numbers: 52.40.Nk, 52.35.Mw, 05.10.Gg, 02.50.Ey

I. INTRODUCTION

One of the grand challenge of laser-plasma interaction (LPI) studies is to provide guidance for the design of hohlraum targets on the next generation of laser facilities for ignition attempts[4–6]. Modeling LPI processes in real-size experiments has been recognized as a difficult task. One of the main difficulties is the vast parameter space in electron density, temperature and spatial scales that are typically spanned by an ignition relevant laser-plasma experiment on current laser facilities. This leads to a plethora of (usually coupled) LPI processes such as filamentation, parametric backscattering instabilities and nonlocal heat transport[7]. Another issue is the description of the spatially smoothed laser beams used on all modern facilities, which exhibit intensity structures from the hundreds of microns down to the micron scale[8].

There are two main numerical modeling approaches for LPI. Particle-in-cell or Focker-Plank type codes solve consistently a set of Maxwell-Vlasov-like equations and are limited to short timescales (picoseconds), small plasma volumes (typically one laser speckle) or low dimensionality (1 or 2 dimensions). While 3-dimensional PIC simulations of diffraction limited short pulse experiments are becoming common thanks to increasingly powerful computers, long pulse (nanosecond) ignition scale (cubic millimeter) LPI experiments are still out of reach for such numerical tools. The second approach is to use a fluid-based description of LPI processes. This allows relaxing both spatial and temporal resolutions and no discretization in particle velocity space is required.

We have developed a new target platform to study Laser Plasma Interaction in ignition-relevant condition at the Omega laser facility (LLE/Rochester)[9]. By shooting an interaction beam along the axis of a hydrocarbon-filled hohlraum heated by up to 17 kJ of heater beam energy (1ns square pulses), we were able to create a millimeter-scale underdense (N_e = 6.5% critical) uniform plasma at electron temperatures T_e around 3 keV. The interaction beam, at a wavelength 0f $\lambda_0 = 0.351\mu m$, is delayed by 300 ps (to allow for T_e to reach 2 keV) and we vary its energy between 50 and 400 J. Using a 150 μm CPP and a 1-ns-square pulse, we can vary the intensity between 5 $10^{14} W.cm^{-2}$ and 4 $10^{15} W.cm^{-2}$. Absolutely calibrated backscattering diagnostics measure the backscattered power in the lens (FABS) and outside (NBI), in a 2 nm wavelength range around λ_0 for SBS and between 450 nm and 650 nm for stimulated Raman scattering (SRS). We use the fluid code pF3d[3], which includes a nonlinear hydrodynamics package coupled to a paraxial solver for the laser propagation. Stimulated Brillouin and Raman instabilities are modeled with enveloping in both time and space, using linear kinetic corrections to the fluid limit. Advanced beam smoothing schemes (double polarization, spectral dispersion) are accurately described. Pf3d is massively parallel and scales up to thousands of processors. Modeling a typical Omega LPI experiment requires simulating a plasma volume of 500 x 500 x 2000 m, which requires a few billion numerical cells. A number of steps are necessary in order to confidently compare pF3d simulation results with the measured reflectivities.

II. DESCRIPTION OF OUR MODELING PLATFORM

A. initial conditions: plasma parameters

First we need accurate plasma parameters as input for pF3d. Extensive Thomson scattering measurements[9] in the multispecies plasma (30% C and 70% H atoms) allowed us to measure both the electron and ion temperatures at the center of the target, as well as the density evolution. These time-resolved measurements were compared to HYDRA simulations and show relative insensitivity to the exact heat conduction model employed[2]. We can then directly use HYDRA three-dimensional hydrodynamics maps (electron density N_e and temperature T_e, ion temperature T_i and plasma flow) as initial conditions for pF3d. We perform post-shot HYDRA simulations to account for variation in heater beam energy (typically $< 4\%$) and gas fill pressure ($< 10\%$) between shots. Our goal is to benchmark pF3d in plasma conditions as close to ignition-hohlraum parameters as possible[6]. We chose to simulate the SBS reflectivity around 700 ps after the heater beams are turned on. At this time, the plasma electron temperature is close to 3 keV and the density profile is still uniform. At earlier times, the plasma is too cold and very large SBS reflectivities are measured. At later times the hohlraum gold wall is converging on axis, leading to larger density perturbations and uncertainty in the ion temperature profiles. Figure 1. shows pF3d simulation of the interaction beam propagating through the hohlraum at 700, 800 and 900 ps. One can see that after 800 ps, refraction (and diffraction) of the beam on density gradients becomes the dominant process and the experiment is no longer relevant to large beams propagating through long-scalelength plasmas. At 700 ps, the plasma is mostly uniform both in the longitudinal and transverse direction over the volume of the interaction beam. Figure 2 shows the plasma parameters along the hohlraum axis at 700 ps.

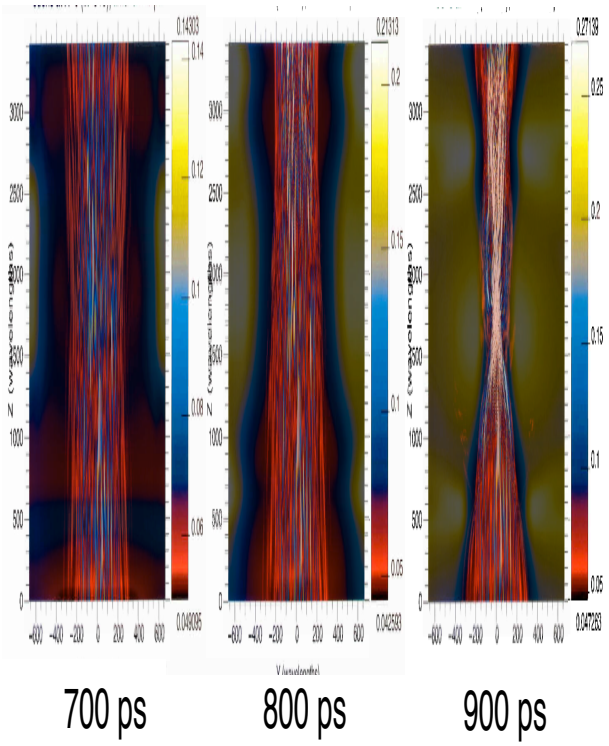

FIG. 1: 3D pF3d simulation of the Interaction beam propagating along the hohlraum axis at 700,800 and 900 ps. After 800 ps, hohlraum closure leads to strong transverse density gradients and refraction and diffraction are dominant over other LPI processes.

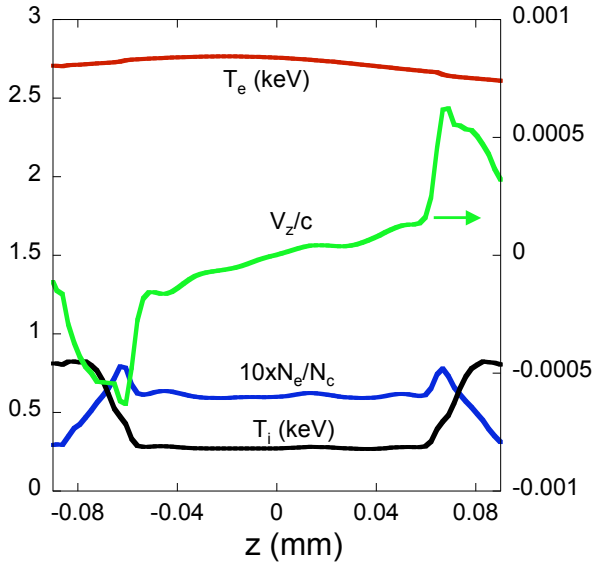

FIG. 2: Plasma parameters at t=700 ps along the hohlraum axis calculated by HYDRA. Electron density, temperature, ion temperature and flow are used as initial conditions for pF3d simulations.

B. Boundary condition: laser beam description

A realistic description of the laser beam is needed. We use the measured continuous phase plate (CPP) phase mask used on the interaction beam and a model for Omega beam aberrations. The beam is focused with an $f/6.7$ circular lens.Figure 3 shows transverse and longitudinal slices through the middle of the resulting beam intensity. The simulation resolves both the envelop of the beam, which is close to a Gaussian with 150 μm FWHM at best focus and the $f/6.7$ speckles at the micron scale. The typical resolution required by the paraxial approximation used for laser propagation is $dx = dy = 1.3\lambda_0$ and $dz = 4\lambda_0$. The plasma volume modeled encompasses more than a billion cells. It is difficult to define an average laser intensity for such a beam, but a benefit of 3D whole beam simulations is that only the beam power

(here in the 100-400 GW range) is needed as an input parameter. For reference, Fig. 3d shows the average intensity function of the distance of propagation. The average is done in each transverse plane over a 30 $\mu m \times 30\ \mu m$ square centered on axis. Another way of defining the intensity for a spatially smoothed beam is to compute the power-averaged intensity and is also plotted. Both are close and can be used in one-dimensionnal analysis of backscattering instabilities.

Additional beam smoothing techniques are equally accurately modeled. When polarization smoothing[10] is used, pF3d solves paraxial equations for each polarization component, with the two speckle patterns being transversally offset in the far field by the experimentally measured shift induced by the PS wedge (15 μm). This offset is much larger than a speckle width ($f\lambda_0 = 2.35\ \mu m$ and effectively decorrelate the speckle patterns while it is small enough to not affect the envelope of the beam (and the average intensity). Smoothing by spectral dispersion (SSD)[11] is modeled using the correct specifications: a 10 Ghz modulator is critically dispersed on a grating to obtain 3Åof bandwidth at 1 μm for our experiment. SSD slightly elongates the focal spot in the direction perpendicular to the offset due to the PS wedge, but the effect on the envelope of the beam is again negligible. This would not be the case if the full bandwidth (11Å) was used.

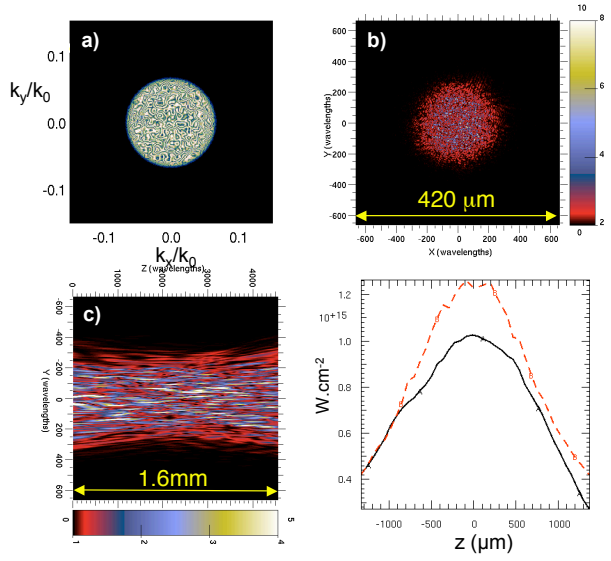

FIG. 3: a) Measured CPP phase mask . b) Focal spot in vacuum as simulated by pF3d. c)Beam intensity profile in a plane parallel to the direction of propagation. d) Laser intensity averaged over 30 μm around the axis (black) and power-averaged intensity (dashed red) as function of the distance of propagation for a power of 100 GW.

C. Stimulated Brillouin backscatter model

A detailed fluid-based model has been developed to describe the response of the plasma to the ponderomotive drive and is described in Ref.[3]. Here we will focus on the details of the SBS model which was dominant in the experiment. pF3D models SBS by solving a system of 3 (5 with PS) coupled waves. The two electromagnetic waves (incident a_0 and backscatterred a_1 light) are solved in the paraxial approximation:

$$\left[\partial_t + v_g\partial_z - \frac{ic^2k_0\nabla_\perp^2}{\omega_0(k_0+\sqrt{k_0^2+\nabla_\perp^2})} + \nu_{ib} + \frac{\partial_z v_g}{2}\right] a_0 = \frac{-i\omega_0}{2n_c}(\delta n_f\ a_0 + \frac{1}{2}\delta n\ a_1) \quad (1)$$

$v_g = c^2k_0/\omega_0$ is the group velocity of light, ν_{ib} the inverse bremstrahlung absorption coefficient and n_c the critical density. The density perturbation has a slow varying component δn_f which is calculated by solving a full set of nonlinear hydrodynamics equations and is responsible for the filamentation and forward Brillouin instabilities, as well as refraction effects. A similar equation is solved for the reflected light a_1.The SBS-driven acoustic wave δn is enveloped in space at $k_a = 2k_0$, but not in time to describe correctly the modified decay regime when the SBS growth rate becomes larger than the acoustic frequency ω_a in high intensity speckles. The resulting differential equation is :

$$(\partial_t + u.\nabla + 2ik_0u_z + \nu_a)^2\delta n + (\omega_a^2 - 2ik_0c_a^2\partial_z - c_a^2\nabla^2)\delta n = \gamma_a a_0 a_1^* \quad (2)$$

The Vlasov-Landau kinetic dispersion relation for SBS-driven ion-acoustic waves at $k = k_a$ is solved at each position in the plasma to account for detuning due to all plasma parameters and the most unstable local solution provides the local acoustic frequency ω_a and Landau damping ν_a. The sound speed is defined as $c_a = \omega_a/k_a$. For the parameters of Fig. 2, at the center of the target, the values are $\omega_a = 13ps^{-1}$ and $\nu_a = 0.15\omega_a$.The coupling coefficient γ_a is obtained by matching the resulting convective amplification to the 1D fully kinetic result. This linear kinetic treatment of SBS-driven acoustic waves provides a correct description of the time evolution of SBS, which is important to correctly model the coupling to other time-dependent LPI processes such as filamentation and SRS and the effect of temporal beam smoothing. Ion-acoustic waves in a multi-ion-species plasma are described by an average (most-unstable) mode. This model also recovers the exact steady-state gain exponent, which is necessary for quantitative comparisons with experiments. It is accurate as long as the ion-acoustic wave amplitude is small enough to neglect kinetic (trapping) and fluid(harmonics, decay,...) nonlinearities and the electron temperature is high enough to neglect collisional corrections to our kinetic approach (such as non-local heat transport). The

later condition is fulfilled in the low density, mid-Z, high temperature experiment (see Fig. 2) described in this letter, as it is in ignition-hohlraum mid-Z plasmas for all current point designs. The validity of the linear assumption for the experiment modeled in this paper is discussed later.

III. MODELING THE EXPERIMENT

A. Whole beam three-dimensionnal simulations

Our approach to simulating SBS consists in using 3D hydrodynamics parameters from an integrated HYDRA simulation of the entire hohlraum as initial conditions for pF3d. This is justified by the separation of time scales between the evolution of the gross hydrodynamics simulated by HYDRA (100 ps) and the LPI processes simulated by pF3d (10 ps). The pF3d simulation is then run for a few tens of picosecond on a plasma volume encompassing the interaction beam, until SBS reaches a statistical steady state. Fig 4. shows that while fast oscillations remains in the reflectivity, a well defined average emerges after 20 picoseconds for various intensities. We define the pF3d reflectivity as the average between 20 ps and 50 ps. The fact that we can start the pF3d simulation using hydrodynamics profiles at 700 ps without prior knowledge of the SBS evolution is justified by an experiment where the interaction beam was delayed by 200 ps and the measured SBS was shown to coincide with the non-delayed measurement[2]: SBS in this CH plasma is in the strongly damped regime and reacts almost instantly (over 10 ps) to local laser-plasma conditions.

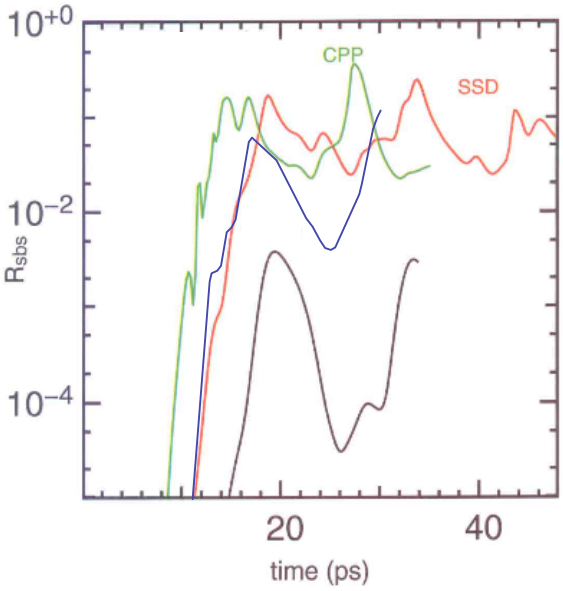

FIG. 4: pF3d calculated SBS reflectivity as function of simulation time for a laser power of 175 GW. (green) is with CPP only, (red) with 3 A of SSD bandwidth and (black) with PS. (blue) corresponds to CPP-only at 130 GW.

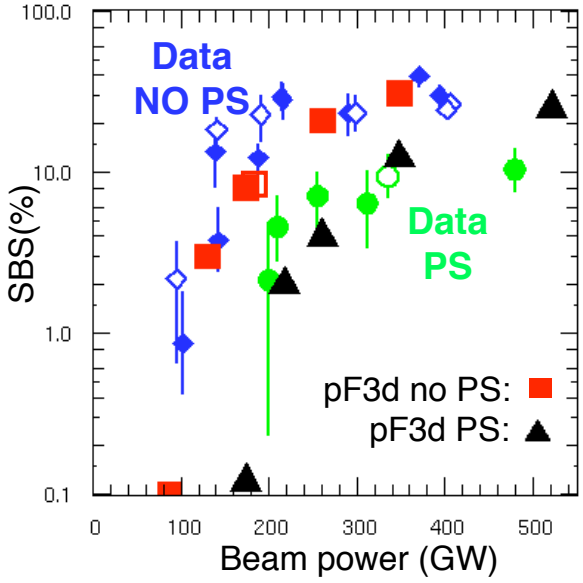

FIG. 5: Measured (blue diamonds and green circles) and calculated (red squares and black triangles) SBS reflectivity as function of laser power at t=700 ps. Both the measurement and simulations show a factor of two increase in the SBS threshold when PS is used. Empty symbols corresponds to measurements and simulations with 3Åof SSD added. pF3d results quantitatively match the measured reflectivity over more than two order of magnitude for all smoothing techniques employed.

Figure 5 shows the measured and simulated SBS reflectivity function of the interaction beam power. It is worth noting again that our modeling doesn't allow for any free parameter: laser and plasma parameters used as boundary and initial conditions are given by measurements or integrated simulations validated by measurements, while the SBS model is closed and derived from first principle linearized equations. Pf3d SBS reflectivities agree quantitatively with measurements over more than 2 order of magnitudes. It predicts correctly the large increase in the SBS threshold when PS is used, as well as the absence of any measurable reduction of SBS when 3 $\AA$ of SSD is added. The SBS signal simulated is almost entirely contained in the beam f-cone, which is consistent with the negligible amount of backscattered light measured outside of the lens (NBI). As Fig. 4 shows, the reflectivity oscillates regularly with a period of approximately 12 ps. The source of these oscillations can be traced back to a few very intense speckles in the back of the plasma. The light scattered by these speckles, while representing a modest amount of power, acts as a seed for SBS that is amplified through the plasma. The resulting pump depletion happening at the front of the plasma due to this enhanced SBS makes these speckles blink, which leads to oscillations with a period close to four times the transit time of light through the plasma.

This is confirmed by the simulation that shows a localized boost in SBS light at time of peak of the reflectivity associated with a coherent near field (Fig6a), meaning only a few coherent structures (speckles) contribute to the boost. At time of low reflectivity, the growth is uniform through the plasma and the incoherent SBS near field shows contribution from the whole beam (Fig6b).

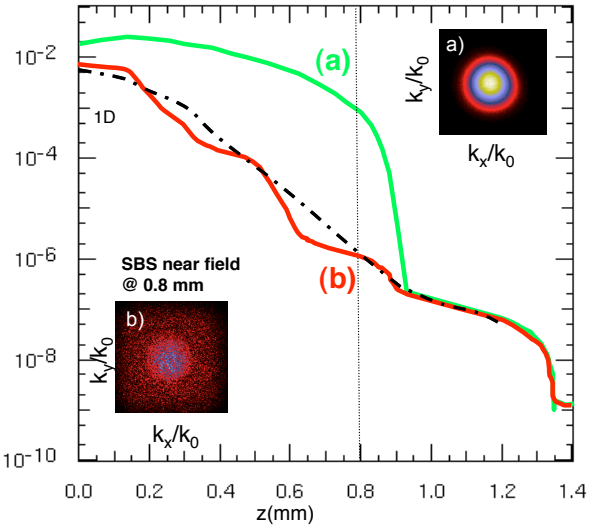

FIG. 6: Transverse average of the reflected SBS light as it grows through the plasma for a laser power of 130 GW. (1, red) corresponds to a time of low SBS (t=22 ps on Fig. 3) while (2,green) corresponds to a time of high SBS (t=28 ps). This oscillation is due to the contribution of one high intensity speckle in the back that seeds the SBS instability through the rest of the plasma. This is indicated by the coherent SBS near field (a) observed in the simulation at the location of fast spatial growth when SBS peaks, as opposed to incoherent contribution (b) from many speckles when SBS is lower.

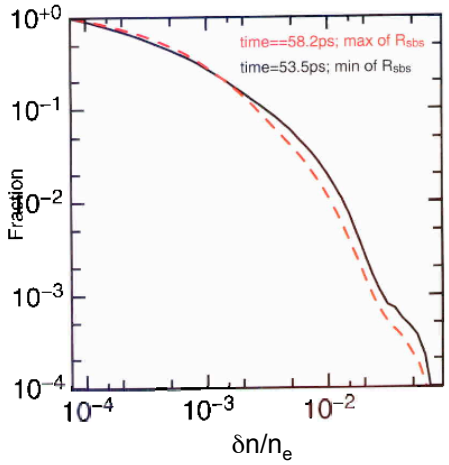

FIG. 7: Statistical distribution of the SBS-driven acoustic wave amplitude $\delta n/n_e$ in the transverse plane of peak average amplitude, for a laser power of 150 GW. The reflectivity was about 8% while wave amplitudes mostly remain in the linear regime.

B. Validity of the linear approximation

The validity of our description of SBS-driven ion-acoustic waves relies on their amplitude remaining small. To quantify this, we have computed the distribution of the wave amplitude $\delta n/n_e$ in a transverse plane close to the entrance of the plasma, where the average amplitude peaks (as the instability grows from the back of the plasma). This is shown in Figure 7. For a laser power of 150 GW and smoothing with CPP only, a reflectivity of about 8% was calculated and we find that 1% (resp. 10%) of the transverse plane is occupied by waves with amplitudes above 1% (resp. 0.3%). The maximum amplitude observed is 3%. Fluid nonlinearities scale usually with $(\delta n/n_e)^2$ and are thus negligible[12, 13]. These amplitudes are also well below the two-ion decay instability threshold $\delta n/n_e > 4\nu_a \approx 60\%$[14] and the wave-breaking limit. Trapping of electron or hydrogen ions in the SBS-driven ion-acoustic wave could lead to a change in Landau damping and a frequency shift[**?**]. The frequency shift induced by electron trapping scales as $\delta\omega/\omega_a \approx 0.2(\delta n/n_e)^{0.5}$ and a similar result is expected for trapping of hydrogen ions. This is a 1% effect for $\delta n/n_e = 0.3\%$ and is much smaller than the linear damping rate ν_a, thus negligible. The last effect could be a reduction of Landau damping in intense speckles. By comparing the bouncing period of protons in an acoustic wave with the transit time of a proton crossing a speckle and with the detrapping timescale due to H-C collisions, one finds that trapping of protons could occur for $\delta n/n_e$ as low as 0.3% with the parameters of Fig. 2. Thus up to 10% of the plasma at the front of the target could be subject to trapping effect (this is still less than 1% of the overall simulation volume). One could then question the validity of our SBS model above 150 GW for CPP-only (and above 300 GW for CPP+PS), but as reflectivities are already large and the physics is dominated by whole-beam pump depletion, the experimental measurement is not discriminative. Nonlinear saturation effects missing in our model could also explain the discrepancy observed at very high power (Fig. 5 around 500 GW). We are not claiming that our modeling tools are accurate at such high intensity and large reflectivities.

C. Polarization smoothing

We turned off the filamentation instability in a few simulations and while the reflectivity was reduced near threshold, the overall result was very close to Fig.5. This is consistent with the high electron temperature and moderate laser intensity, which results in weak self-focusing of speckles and limited change to the beam contrast. Thus the factor of 2 increase in the SBS thresh-

old when PS is used is not due to a control of the filamentation instability[16–18] but to a direct mitigation of the SBS growth. Indeed, the average laser intensity doesn't exceed the so-called critical intensity for SBS (corresponding to an e-fold amplification over one speckle length) until very large reflectivity are measured. In this regime of low amplification over any speckle, a single row of speckles can act as an enhanced noise source but has a negligible contribution in the overall reflectivity, which is determined by amplification over many successive rows. When PS is used, on average only one or the other polarization is amplified over any speckle, which leads in the limit of small amplification per speckle to a reduction of 2 of the overall gain exponent throughout the whole plasma. This is observed both in the experiment and in the simulations.

D. Smoothing by spectral dispersion

Using 3 Åof SSD bandwidth has no significant effect on SBS, both in the experiment and in simulations. This can be expected in this strongly damped regime where the damping rate ν_a is almost 10 times larger than the inverse correlation time introduced by the laser bandwidth[19, 20]. Previous observations of SBS reduction through control of filamentation by SSD[21] does not apply to this high Te, moderate intensity experiment, as noted before.

IV. CONCLUSION

While developing a general predictive modeling capability for LPI remains a challenge, we have made a significant step towards that goal by using a detailed description of the plasma conditions and the laser beam intensity pattern as input to full 3D fluid-based LPI simulations done with our massively parallel code pF3d. This experimental validation is for now limited to stimulated Brillouin backscatter in a regime where kinetic and fluid nonlinearities are not expected to play a significant role (long hot plasma at moderate density and laser intensity). This is a regime of interest for forthcoming attempts at ignition on NIF and LMJ.

This work was performed under the auspices of the U.S. Department of Energy by Lawrence Livermore National Laboratory in part under Contract W-7405-Eng-48 and in part under Contract DE-AC52-07NA27344.

[1] Froula, D. H. *et al.*, Phys. Rev. Lett. 98, 085001 (2007).
[2] Meezan, N. B. *et al.*, Phys. Plasmas **14**, 056304 (2007)
[3] Berger, R. L. *et al.*, Phys. Plasmas **5**, 4337 (1998)
[4] Moses, E. I. and Wuest C. R. Fusion Sci. Tech. 47, 314-322 (2005).
[5] Cavailler, C. Fusion 47, B389-B403 (2005).
[6] Lindl, J. D. *et al.*, Phys. Plasmas 11, 339 -491 (2004).
[7] Kruer,W. L. The Physics of Laser Plasma Interaction (Addison-Wesley, New York, 1988)
[8] Still, C. H. et al. Phys. Plasmas 7, 2023-2032 (2000).
[9] Froula, D. H. *et al.*, Phys. Plasmas **14**, 055705 (2007)
[10] Tsubakimoto, K. *et al.*, Opt. Commun. 91, 9-12 (1992).
[11] Skupsky, S. *et al.*, J. Appl. Phys. 66, 3456-3462 (1989).
[12] Heikkinen, J. A. *et al.*, Phys. Fluids 27, 707-720 (1984).
[13] Rozmus, W. *et al.*, Phys. Fluids B 4, 576-593 (1992).
[14] Niemann, C. *et al.*, Phys. Rev. Lett. 93, 045004 (2004)
[15] Riconda, C. *et al.*,Phys. Rev. Lett. 94, 055003 (2005).
[16] Lefebvre, E. *et al.*, Phys. Plasmas 5, 2701- 2705 (1998)
[17] Berger, R. L. *et al.*, Phys. Plasmas 6, 1043 (1999)
[18] Fuchs, J. *et al.*, Phys. Rev. Lett. 84, 3089 (2000)
[19] Divol, L. Phys. Rev. Lett. 99, 155003 (2007).
[20] Mounaix, Ph., Phys. Rev. Lett. 85, 4526 (2000).
[21] Glenzer, S. H. Nature Physics, 10.1038,nphys709